



## Comprehensive learning bat algorithm for optimal coordinated tuning of power system stabilizers and static VAR compensator in power systems

Bousaadia Baadji , Hamid Bentarzi & Azzeddine Bakdi

To cite this article: Bousaadia Baadji , Hamid Bentarzi & Azzeddine Bakdi (2020) Comprehensive learning bat algorithm for optimal coordinated tuning of power system stabilizers and static VAR compensator in power systems, Engineering Optimization, 52:10, 1761-1779, DOI: [10.1080/0305215X.2019.1677635](https://doi.org/10.1080/0305215X.2019.1677635)

To link to this article: <https://doi.org/10.1080/0305215X.2019.1677635>



Published online: 05 Nov 2019.



Submit your article to this journal [↗](#)



Article views: 81



View related articles [↗](#)



View Crossmark data [↗](#)



Citing articles: 2 View citing articles [↗](#)



# Comprehensive learning bat algorithm for optimal coordinated tuning of power system stabilizers and static VAR compensator in power systems

Bousaadia Baadji<sup>a</sup>, Hamid Bentarzi<sup>a</sup> and Azzeddine Bakdi<sup>b</sup>

<sup>a</sup>Signals and Systems Laboratory, Institute of Electrical and Electronics Engineering, University M'Hamed Bougara of Boumerdes, Boumerdès, Algeria; <sup>b</sup>Department of Mathematics, University of Oslo, Oslo, Norway

## ABSTRACT

This article presents a novel comprehensive learning bat algorithm (CLBAT) for the optimal coordinated design of power system stabilizers (PSSs) and static VAR compensator (SVC) for damping electromechanical oscillations in multi-machine power systems considering a wide range of operating conditions. The CLBAT incorporates a new comprehensive learning strategy (CLS) to improve microbat cooperation; location updating is also improved to maintain the bats' diversity and to prevent premature convergence through a novel adaptive search strategy based on relative travelled distance. In addition, the proposed elitist learning strategy speeds up convergence during the optimization process and drives the global best solution towards promising regions. The superiority of the CLBAT over other algorithms is demonstrated via several experiments and comparisons through benchmark functions. The developed algorithm ensures convergence speed, credibility, computational resources and optimal tuning of PSSs and SVCs of multi-machine systems under different operating conditions through eigenanalysis, nonlinear simulation and performance indices.

## ARTICLE HISTORY

Received 27 January 2019  
Accepted 30 August 2019


## KEYWORDS

Power system stabilizer; static VAR compensator; comprehensive learning; adaptive search strategy; elitist learning

## 1. Introduction

Electromechanical oscillations impose great challenges in modern power systems since they limit the maximum power transfer capability and deteriorate the system stability (Kundur, Balu, and Lauby 1994). Power system stabilizers (PSSs) are thus widely employed to damp such electromechanical oscillations and restore operational stability. However, under some operating conditions, PSSs fail to provide enough damping, especially for inter-area oscillation modes. The emergence of flexible alternating current transmission systems (FACTS) provides an alternative solution to improve the system damping (Bian *et al.* 2016; Shahgholian and Movahedi 2016). Among the various types of FACTS, the static VAR compensator (SVC) is one of the most common devices used for this purpose. Although the SVC is basically employed for regulating the bus voltage, studies have demonstrated that it can also boost the system stability (Mondal, Chakrabarti, and Sengupta 2012; Abido and Abdel-Magid 2003).

The simultaneous design of controllers in power systems is based on the optimization of complex non-differentiable problems, which generally causes serious challenges for the application of traditional compensation strategies.

**CONTACT** Bousaadia Baadji  [lss@univ-boumerdes.dz](mailto:lss@univ-boumerdes.dz); [b\\_baadji@yahoo.com](mailto:b_baadji@yahoo.com)

This article has been corrected with minor changes. These changes do not impact the academic content of the article.

Several analytical approaches, based on traditional control theory, have been used to design robust power system controllers, such as  $H_\infty$  optimization techniques (Yang 1997), structured singular value (Castellanos, Messina, and Sarmiento 2008) and bilinear matrix inequalities (de Campos, da Cruz, and Zanetta 2014). These designs face the common problems of the selection of weighting functions, pole-zero cancellation and their requirements for higher order controllers which make them less common in applications. Adaptive control techniques have also been proposed (Nechadi *et al.* 2012; Hussein *et al.* 2010), where the controllers are designed with quickly adjustable parameters according to the changes in the system parameters. However, since power systems are time varying, the implementation costs of real-time adaptive controllers are high as the on-line parameter identification process is computationally heavy, particularly if optimal design is considered. Alternatively, artificial neural networks (ANNs) have been adopted in the design of PSSs (Tofighi *et al.* 2015; Mahabuba and Khan 2009). ANN-based controllers can significantly improve the system performance, but at the price of their exploding computation capacity with large amounts of training data and long training time. Sambariya and Prasad (2015) and Bouchama *et al.* (2016) used fuzzy logic control (FLC) for the design of PSSs to address the inaccuracies and uncertainties in the system model. However, extensive refinements to FLC are required before its application.

Modern studies have employed population-based algorithms to overcome these problems and achieve optimal settings for robust performance. The teaching–learning algorithm with chaotic strategy (Farah, Guesmi, and Abdallah 2017) was adopted in the coordinated design of a thyristor-controlled series capacitor (TCSC) and PSSs. The small signal stability of a power system was enhanced through the tuning of SVC and TCSC via the particle swarm optimization algorithm (Mondal, Chakrabarti, and Sengupta 2012). The flower pollination algorithm was employed for the robust design of SVC in a power system (Abdelaziz and Ali 2015). The gravitational search algorithm was combined with a gradient local search method (Peres, Silva Júnior, and Filho 2018) and employed for various types of PSS design. The optimal design of PSSs was proposed via the cuckoo search algorithm (Abd-Elazim and Ali 2016b). The bacteria foraging algorithm was adopted for the coordinated tuning of SVC and PSSs (Abd-Elazim and Ali 2012). The shuffled frog-leaping algorithm (Darabian, Mohseni-Bonab, and Mohammadi-Ivatloo 2015) was proposed to improve power system stability through the optimal tuning of SVC. Despite the many research studies in the field, an optimal solution to this optimization problem does not exist in a closed form, which allows for future improvements.

The bat algorithm (BA) (Yang and Gandomi 2012) is a metaheuristic algorithm inspired by the echolocation behaviour of microbats. The BA employs a varying frequency, with increasing pulse emission rates and decreasing loudness of bats to search for and locate the global best solution (gbest). The key advantage of the BA is its higher accuracy in finding the optimal solution owing to the echolocation capacity of its microbats, which can efficiently find their prey, distinguish it from local candidates and precisely determine its location. However, the BA is still prone to premature convergence and trapping into local optima; this issue, in addition to the unsatisfied balance between exploration and exploitation, requires further improvements which will be introduced along with novel developments in this article.

Accordingly, variants of the BA have been proposed in an attempt to enhance its optimization performance. Liu *et al.* (2018) enhanced the BA's local search capability based on chaotic initialization of the population, position updating via a nonlinear decreasing time factor, and hybridization with an external optimization algorithm. Meng *et al.* (2015) proposed compensation for the Doppler effect in echoes and the foraging habitat of bats by further mimicking the bats' behaviour. Four strategies were also proposed by Bahmani-Firouzi and Azizipanah-Abarghooee (2014) for updating the bats' velocities, in which an accumulator for each strategy was computed and used to determine the probability of selecting that strategy. Saad *et al.* (2019) utilized a kriging surrogate model to solve computationally expensive black-box optimization problems. Despite these various efforts, the possibilities for enhancement remain, as there is no algorithm that is ultimately perfect, as indicated by the 'no free lunch' theorem (Ho and Pepyne 2002).

The utilization of the information of individuals from previous iterations for the improvement of metaheuristic algorithms has proved to be an efficient strategy (Wang and Tan 2017). As an example, the modified biogeography-based optimization (BBO), proposed by Jalili, Hosseinzadeh, and Taghizadieh (2016), adopted a strategy in which elite individuals are transferred from the previous generation to the current one, where they are reused in combination with the new individuals. The bare bones artificial bee colony (ABC) algorithm (Gao *et al.* 2015) improves the search ability through a Gaussian search equation that exploits the information on the best individual to generate a new candidate in the onlooker phase. In this employed bee phase, a parameter adaptation strategy and a fitness-based neighbourhood mechanism exploit the information from the previous search and from the best individuals, respectively. The comprehensive learning particle swarm optimizer (CLPSO) (Liang *et al.* 2006) incorporates a comprehensive learning strategy (CLS) to improve its efficiency via cooperative learning based on the exchange of information from previous iterations between all the particles in the swarm.

Motivated by these significant improvements, a novel CLS is developed as an extension to the traditional BA, which ignores the use of previous information from other individuals except for the best candidate. A comprehensive learning bat algorithm (CLBAT) is introduced to improve and control the search memory during the optimization process, in which the current location can potentially learn from the previous best locations of all individuals, and is not restricted to the global best location as in the original BA. In addition, an elitist learning strategy (ELS) is proposed to push gbest out of regions of local optima. Moreover, a new adaptive search strategy is introduced to control the travelled distance of each microbat as an indicator of the tendency to either exploit or explore for new solutions; this plays a positive role in speeding up the optimization process, which is a known limitation of the original BA. The proposed algorithm is first tested against benchmark functions, in which it shows superior performance. CLBAT is then employed for the coordinated design of PSSs and SVC controllers for a two-area four-machine (TAFM) system under different operating conditions. The performance of the obtained controllers is evaluated through eigenvalue analysis, nonlinear simulation and indices, where the proposed controllers effectively damp out the electromechanical oscillations and attain robust performance for all of the considered conditions.

This article introduces the CLBAT. This novel algorithm is tested against the benchmark test functions and then employed in the coordinated design of PSSs and SVC. The obtained results and relevant comparisons are discussed and concluding remarks are drawn, together with proposals for future work.

## 2. Problem formulation

### 2.1. Power system modelling

The power system model is generally described using a set of nonlinear differential equations (Kundur, Balu, and Lauby 1994):

$$\dot{x} = f(x, u) \quad (1)$$

where  $x$  is the vector of the system states, including the generators, loads and other controllers such as SVCs and PSSs, and  $u$  is the vector of the system inputs. A full description of the set of equations governing the system operation is available in the literature (Sauer and Pai 1998).

For a given operating point, the linearized model is represented in the state-space approach as:

$$\dot{x} = Ax + Bu \quad (2)$$

where  $A$  is the state matrix that determines the system eigenvalues, and is obtained by  $\frac{\delta f}{\delta x}$  at a given operating point, and  $B$  is the input matrix that is equal to  $\frac{\delta f}{\delta u}$ .

The damping ratio  $\zeta$  that corresponds to a single eigenvalue  $\lambda$  is given by:

$$\zeta = \frac{-\text{real}(\lambda)}{\sqrt{\text{real}(\lambda)^2 + \text{imag}(\lambda)^2}} \tag{3}$$

### 2.2. PSS modelling

The main functions of a PSS are to improve the system stability and mitigate the electromechanical oscillations by modulating the automatic voltage regulator output. The conventional PSS (Figure 1) is adopted in this work. It is composed of a stabilizer gain  $K_s$ , washout block and lead-lag compensators. Its input is the rotor speed deviation ( $\Delta\omega$ ).

The role of  $K_s$  is to specify the amount of damping injected to mitigate the system oscillations. The washout block is a high-pass filter that prevents the direct current (DC) component of the input signal from affecting the terminal voltage; hence, the washout time constant  $T_w$  is set to 10 s. The two lead-lag blocks, characterized by time constants  $T_1, T_2, T_3$  and  $T_4$  (in seconds), are used to compensate for the phase lag between the input and the output of the PSS.

### 2.3. SVC modelling

The SVC (Figure 2) is a shunt-connected static VAR generator that consists of a fixed capacitor  $C$  in parallel with a thyristor-controlled rectifier. The SVC maintains a fixed bus voltage and boosts the system stability. Its contribution in damping such oscillations is significantly improved by adding an auxiliary controller, usually a lead-lag compensator, to the voltage control loop of the SVC.

The block diagram of the SVC shown in Figure 3 presents the thyristor firing control system characterized by gain  $K_r$  and time constant  $T_r$ , and an auxiliary controller characterized by gain  $K_{svc}$  and two lead-lag blocks.

The firing angle of the thyristor adjusts the SVC output, which is the equivalent susceptance, to control the bus voltage.

The state-space representation of the SVC controller is therefore given by:

$$\dot{B}_{svc} = \frac{1}{T_r}(-\dot{B}_{svc} + k_r(V_{ref} - V_t + V_s)) \tag{4}$$

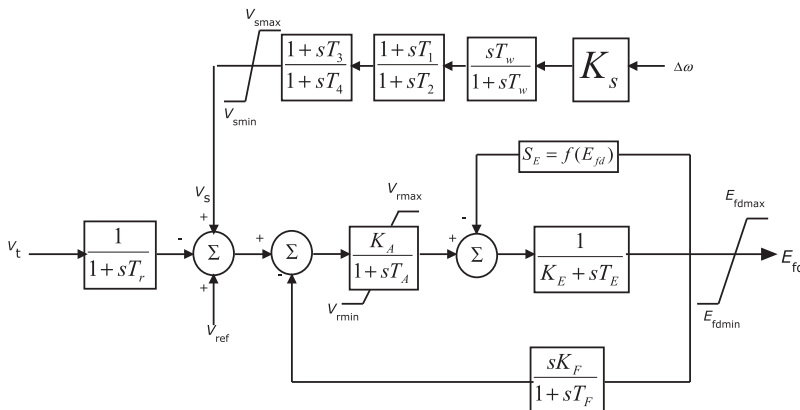


Figure 1. Block diagram of the power system stabilizer (PSS) and excitation system.

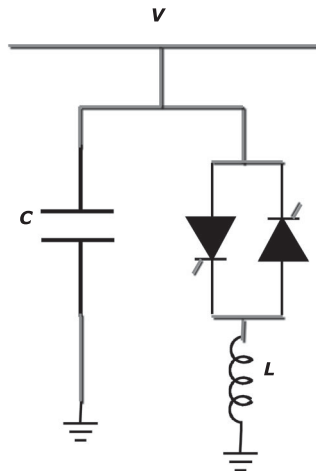


Figure 2. Static VAR compensator (SVC) model.

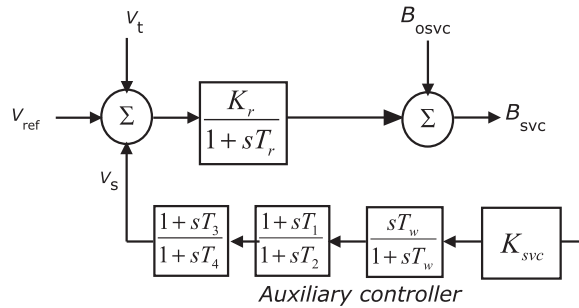


Figure 3. Block diagram of the static VAR compensator (SVC).

### 3. Bat algorithm

#### 3.1. Original BA

The BA is a metaheuristic algorithm that has been applied successfully for solving various optimization problems such as robust design of multiple trailing edge flaps for helicopter vibration reduction (Mallick, Ganguli, and Bhat 2015), the redundancy allocation problem (Talafuse and Pohl 2016), maximum power point tracking in photovoltaic systems (Oshaba, Ali, and Elazim 2017) and tuning proportional–integral controllers to design the load frequency controller (Abd-Elazim and Ali 2016a). The echolocation behaviour of bats gives them the ability not only to localize their prey but also to discriminate it from other objects. Microbats use a type of sonar, called echolocation, to detect prey; they emit a sound pulse with loudness that varies from the loudest when searching for prey to a quieter base when approaching the prey. Most bats use short frequency-modulated signals for echolocation.

The BA is formulated by idealizing the echolocation behaviour of bats using the following approximate rules:

- (1) All bats use echolocation to sense the distance of the prey and obstacles, and to discriminate between them.

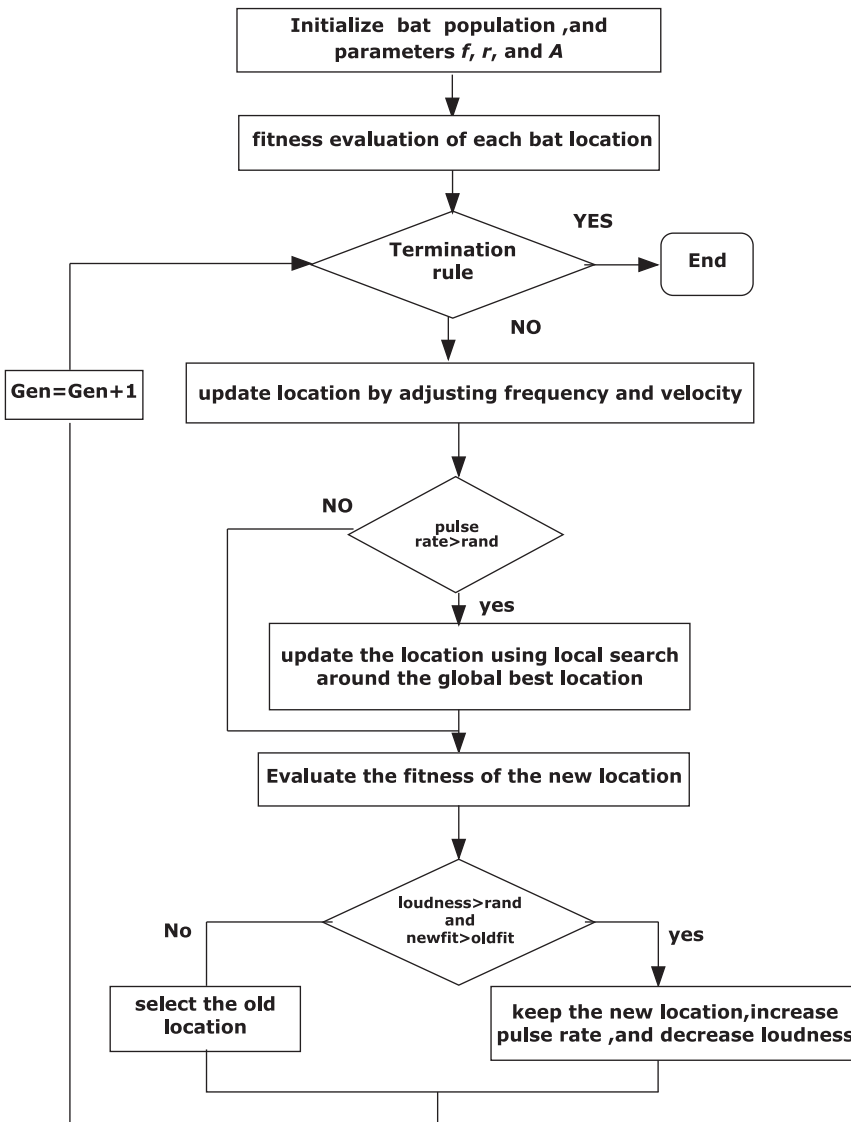


**Figure 4.** Bat algorithm (BA) flowchart.

- (2) The bats fly randomly with velocity  $v_i$  at position  $x_i$  with a fixed frequency  $f_{\min}$ , varying wavelength  $\lambda$  and loudness  $A_0$  to search for their prey. They adjust the frequency of the emitted pulses, and the rate of pulse emission  $r$  in the range of  $[0, 1]$ , depending on the proximity of their target.
- (3) The loudness varies from a large  $A_0$  to a minimum value  $A_{\min}$ , while the frequency varies within the range  $[f_{\min}, f_{\max}]$ .

### 3.1.1. BA design procedures

The basic procedure of the BA is shown in Figure 4, which can be summarized through the following steps.

In the initial phase, the positions  $x_i$  and velocities  $v_i$  of the bats are randomly distributed in the  $D$ -dimensional search space, and they are updated in each iteration according to the following

equations:

$$f_i = f_{\min} + (f_{\max} - f_{\min})\beta \quad (5)$$

$$v_i^t = v_i^{t-1} + (x_i^t - x_g^t)f_i \quad (6)$$

$$x_i^t = x_i^{t-1} + v_i^t \quad (7)$$

where  $\beta \in [0, 1]$  is a uniform random vector,  $x_g^t$  is the current gbest, and  $f_{\max}$  and  $f_{\min}$  are the values of the maximum and minimum frequencies, respectively.

For each bat, its pulse rate is less than a uniform random number within  $[0, 1]$ . The local search using random walk is performed to generate a new solution around the current gbest.

$$x_{\text{new}} = x_g^t + \varepsilon A^t \quad (8)$$

where  $\varepsilon \in [-1, 1]$  represents a uniform random number, and  $A^t$  stands for the mean of the loudness of all bats at iteration  $t$ . As the number of iterations increases, the bats move closer to their target, and the loudness is decreased while the pulse rate emission is increased. Hence, the update for these parameters is given as:

$$A_k^{t+1} = \alpha A_k^t \quad (9)$$

$$r_k^{t+1} = r_k^0(1 - e^{-\gamma t}) \quad (10)$$

where  $\alpha$  is a constant selected such that  $0 < \alpha < 1$ , and  $\gamma$  is a positive constant.

### 3.2. Comprehensive learning bat algorithm

#### 3.2.1. Comprehensive learning strategy

The original BA relies only on its gbest to update the bats' velocities at each iteration, and eventually all bats are attracted to the region of gbest that is expected to be the global optimum. However, if gbest is stuck in the local optimum region, the bats are trapped in that local optimum. To overcome this deficiency, the CLBAT employs an information-sharing strategy known as CLS (Liang *et al.* 2006), in which the information stored about the bats' previous best locations serves to improve the performance by increasing the diversity through the adopted velocity updating strategy:

$$v_{di}^t = w.v_{di}^{t-1} + r_{di}.d.(x_{di}^t - bx_{di}^t)f_{di} \quad (11)$$

where  $v_{di}^t$  is the velocity of the  $d$ th dimension of the  $i$ th bat at iteration  $t$ ; similarly,  $x_{di}^t$  and  $bx_{di}^t$  are the current location and the best location of the  $d$ th dimension of the  $i$ th bat at iteration  $t$ , and  $f_{di}$  is the frequency of that dimension.  $r_{di}$  is a random number uniformly distributed between 1 and 0, and  $d$  is an inertia weight.  $W$  is the inertia weight, which is decreased linearly from  $W_{\max}$  to  $W_{\min}$ :

$$w = (w_{\max} - w_{\min}).\left(1 - \frac{\text{iter}}{\text{iter}_{\max}}\right) + w_{\min} \quad (12)$$

$W$  is used to balance between the global and local searches. It is started with a large inertia weight to rapidly direct the algorithm towards a global search, and decreases as the number of iterations increases, to encourage exploitation during the convergence towards the global solution.

To illustrate the advantages of the CLBAT, consider the problem of minimizing a function  $f(X)$  with dimension  $D$ , where  $X = (x_1, x_2, \dots, x_D)$  and  $X_G = (x_{G1}, x_{G2}, \dots, x_{GD})$  denote a solution in the search space and the global optimum, respectively. An arbitrary solution  $X_C$  with poor fitness  $f(X_C)$  could discover the  $i$ th dimension's solution such that  $x_{Ci} = x_{Gi}$ . To keep and transfer this beneficial information, the CLBAT enables the sharing of information among bats through the CLS, which



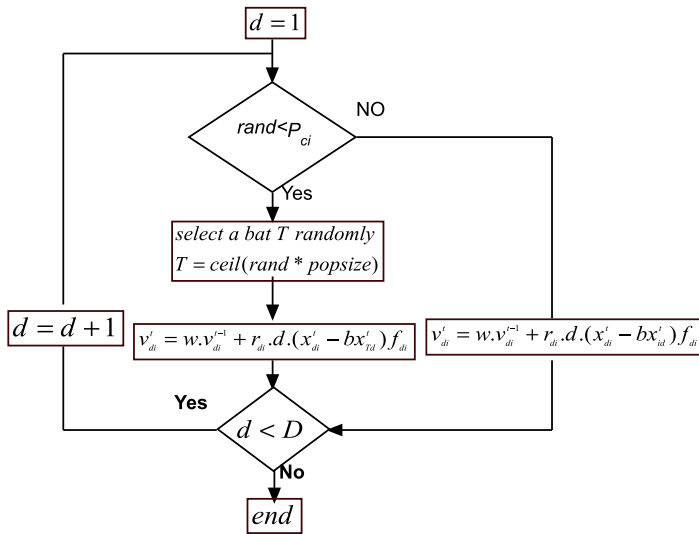


Figure 5. Velocity update for bat  $i$  at iteration  $t$ .

is based on two features: (1) only the sharing of previous best information is allowed; and (2) a learning probability  $P_{ci}$  controls the updating of velocity at a dimension  $d$  using the dimension of a randomly selected best location  $bx_{Td}$  in the case where  $P_{ci}$  is less than a randomly generated number; otherwise, it is updated using its own best location  $bx_{id}$ . This velocity-updating strategy is demonstrated in Figure 5.

The learning probability is crucial in the determination of CLBAT performance, and is given as:

$$P_C = (P_{\max} - P_{\min}).\left(1 - \frac{iter}{iter_{\max}}\right)^2 + P_{\min} \tag{13}$$

The nonlinear  $P_c$  is more adequate for obtaining the proper balance between the exploration and the exploitation states of the CLBAT. In the early stage, relatively high values of  $P_c$  encourage the microbats to learn from their own previous information through the use of their best locations, because the CLBAT is in the exploration phase (high  $w$ ) since the sharable information is very limited at this stage. In the final stage, however, the relatively low  $P_c$  encourages information sharing, in which a bat will more probably learn from other bats' best locations, because the CLBAT is in the convergence state where more useful information is discovered, especially about the global optimum in some dimensions. Therefore, the controlled information sharing among the bats allows useful propagation within the population.

### 3.2.2. New search method

The conventional search strategy of the BA is locally limited around  $g_{best}$  based on the mean of the loudness. Because of this high dependence, however, the loudness control of the search radius is not sufficient to speed up the convergence rate of the algorithm. Although the distribution of the bat's new locations varies dynamically during the optimization process, the new locations are often far from the old locations in the exploration state, and very close in the final stage, owing to the adopted position-updating strategy in the CLBAT. Hence, the difference between the bat's new and old locations has the same behaviour as the loudness, as it is large at the beginning and slowly decreases during the optimization process. The new search method is suitable for adaptively refining  $g_{best}$  for exploration and convergence states. The new search protocol is defined as:

$$Nx_i^{t+1} = x_g^t + A_i.rand1.(Nx_i^t - x_i^t) \tag{14}$$

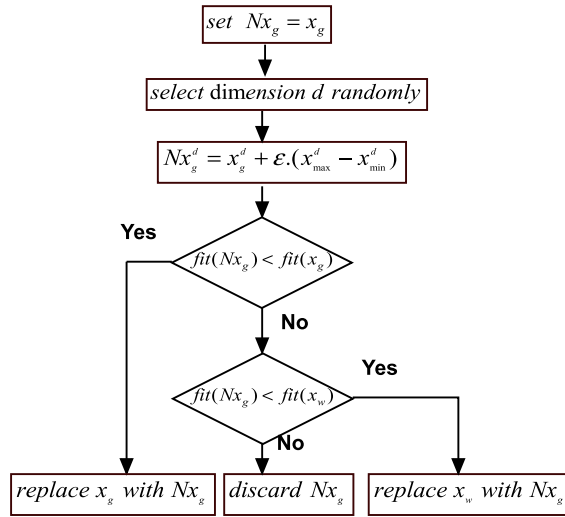


**Figure 6.** Modified elitist learning strategy.

where  $Nx_i^t$  represents the bat’s new location,  $x_g^t$  is the current gbest, and  $rand1$  is a random number drawn from a standard normal distribution.

The new search strategy adaptively controls the search around gbest depending on the last travelled distance from the bat’s old location to its new location. Since  $Nx_i^t$  is far from  $x_i^t$  in the exploration phase, the search around gbest is performed with large travelled steps and more potential locations may be discovered. In contrast, the distance between  $Nx_i^t$  and  $x_i^t$  is minimal at the final stage and the search only refines gbest.

**3.2.3. Modified elitist learning strategy**

A modified ELS (Figure 6) is adopted as a jumping-out mechanism that updates gbest at randomly selected dimensions to move it to better regions and helps it to escape local optima. One dimension of a gbest solution is selected randomly to undergo modifications to preserve the main structure of gbest, since many dimensions of gbest contain the information about the global optimum. The modified ELS is given as:

$$Nx_g^d = x_g^d + rand2.(x_{max}^d - x_{min}^d) \tag{15}$$

where  $rand2$  is a random number from a uniform distribution within  $[-1, 1]$ .

It is worth noting that in the proposed ELS (Zhan *et al.* 2009),  $Nx_g^d$  replaces gbest if its fitness is better; otherwise, it replaces the worst fitness particle  $X_w$ . Notice that this strategy may slow down the convergence if the fitness of  $Nx_g$  is worse than that of  $X_w$ ; for that reason,  $Nx_g$  is kept in the modified ELS only if its fitness is better than the fitness of gbest or  $X_w$ .

**4. Test functions**

The performance of the developed CLBAT is first tested on a set of benchmark functions with various properties to assess its ability in exploring the region of search and jumping over regions of a local optimum. Table 1 lists the details of each test function with its corresponding name, optimization function, range of the search space and the maximum tolerance value to accept an optimization solution.

The resulting performance of the CLBAT is also compared with the ABC algorithm (Karaboga and Basturk 2007), original BA (Yang and Gandomi 2012) and BBO (Simon 2008). For a robust and

**Table 1.** Test numerical functions.

Name	Formula	Range	Global $f_{\min}$	Accept
Sphere	$f_1(x) = \sum_{i=1}^D x_i^2$	$[-100,100]$	0	1e-2
Zakharov	$f_2(x) = \sum_{i=1}^D x_i^2 + \left(\sum_{i=1}^D 0.5x_i\right)^2 + \left(\sum_{i=1}^D 0.5x_i\right)$	$[-10,10]$	0	1e-2
Sum square	$f_3(x) = \sum_{i=1}^D (ix_i)^2$	$[-100,100]$	0	1e-5
Rastrigin	$f_4(x) = \sum_{i=1}^D (x_i^2 - 10 \cos(2\pi x_i)) + 10$ $f_5(x) = \sum_{i=1}^D (y_i^2 - 10 \cos(2\pi y_i)) + 10$	$[-5.12,5.12]$	0	1e-5
Non-continuous Rastrigin	$y_i = \begin{cases} x_i &  x_i  < 0.5 \\ \text{round}(2x_i)/2 &  x_i  \geq 0.5 \end{cases}$	$[-5.12,5.12]$	0	1e-5
Rosenbrock	$f_6(x) = \sum_{i=1}^{D-1} (100(x_i^2 - x_{i+1})^2 + (x_i^2 - 1)^2)$	$[-2.048,2.048]$	0	5
Schwefel 2.21	$f_7(x) = \max\{ x_i , 1 \leq i \leq D\}$	$[-100,100]$	0	1e-2
Schwefel 2.22	$f_8(x) = \sum_{i=1}^D  x_i  + \prod_{i=1}^D  x_i $	$[-10,10]$	0	1e-2
Levy	$f_9(x) = \sin^2(\pi y_i) + \sum_{i=1}^{D-1} (y_i - 1)^2(1 + 10\sin^2(\pi y_i + 1))$ $+ (y_D - 1)^2(1 + \sin^2(2\pi y_D))$ $y_i = 1 + \frac{1}{4}(x_i - 1)$ $f_{10}(x) = \frac{\pi}{D}[10\sin^2(\pi y_1) + \sum_{i=1}^{D-1} (y_i - 1)^2$	$[-10,10]$	0	1e-5
Penalized 1	$\times (1 + 10 \sin(\pi y_{i+1})) + (y_D - 1)^2$ $+ \sum_{i=1}^D u(x_i, 10, 100, 4)$	$[-50,50]$	0	1e-5
Penalized 2	$y_i = 1 + \frac{1}{4}(x_i + 1); u_{x_i,a,k,m} = \begin{cases} k(x_i - a)^m & x_i > a \\ 0 & -a \leq x_i \leq a \\ k(-x_i - a)^m & x_i < -a \end{cases}$ $f_{11}(x) = \frac{\pi}{D}[10\sin^2(3\pi x_1) + \sum_{i=1}^{D-1} (x_i - 1)^2$ $\times (1 + 10 \sin(3\pi x_{i+1})) + (x_D - 1)^2$ $+ \sum_{i=1}^D u(x_i, 5, 100, 4)$	$[-50,50]$	0	1e-5

fair comparison of the results, the algorithms are tested for 30 independent runs for a sufficient maximum number of fitness evaluations set to 120,000 and with a population size of 40. The means and standard deviations of the proposed algorithms are presented in Table 2. CLBAT outperforms the other algorithms across all the test functions since it reaches accurately the global optimum of functions ( $f_1$ - $f_5$ ) for all the runs with zero mean and standard deviation results. For ( $f_6$ - $f_{11}$ ) the accuracy is very high and much better compared to the other algorithms, as the mean is very close to the global  $f_{\min}$ . Specifically, the results demonstrate that the CLBAT is able to jump out of local solutions through the embedded CLS, modified ELS and adaptive search strategies.

### 5. Controller design using the CLBAT

The modes of oscillations in a linear system are related to its eigenvalues. To improve the power system stability, a multi-objective function is employed to relocate all the eigenvalues within the D-contour (Abdel-Magid and Abido 2003). The latter is characterized by  $\delta_{ij} \leq \delta_o$ , and  $\zeta_{ij} \geq \zeta_o$ , as shown in Figure 7. The values of  $\delta_o$ ,  $\zeta_o$  and the weighting factor  $q$  are empirically set to  $-2.0$ ,  $0.25$  and  $10$ , respectively, based on the system under study to ensure sufficient damping to the electromechanical oscillations. The PSS and SVC parameters are simultaneously tuned using CLBAT to shift all modes within the D-contour over a given range of operating conditions to guarantee a well-damped response over that specified range.

**Table 2.** Results of the comprehensive learning bat algorithm (CLBAT) compared to the state-of-the-art algorithms.

Name		CLBAT	ABC	BA	BBO
Sphere	Mean	<b>00e00</b>	4.6103e-16	1.7617e-06	4.5731e-09
	StdDev	<b>00e00</b>	4.9036e-17	4.6416e-07	5.2354e-09
Zakharov	Mean	<b>00e00</b>	5.0351e-16	6.3080e-05	1.2455e-09
	StdDev	<b>00e00</b>	7.1333e-17	1.6868e-05	4.8086e-09
Sum square	Mean	<b>00e00</b>	5.1222e-16	5.2112e-05	1.3093e-07
	StdDev	<b>00e00</b>	4.2745e-17	1.3938e-05	8.6187e-08
Rastrigin	Mean	<b>00e-00</b>	4.1685e-14	1.4213e02	2.0187e-06
	StdDev	<b>00e-00</b>	2.5567e-14	3.2932e01	2.3970e-06
Non-continuous Rastrigin	Mean	<b>00e00</b>	00e00	1.7249e02	4.2680e00
	StdDev	<b>00e00</b>	00e00	4.9104e01	1.3620e00
Rosenbrock	Mean	<b>2.658e-01</b>	3.6731e00	8.394e-01	2.1166e01
	StdDev	<b>1.0114e00</b>	2.5191e00	1.6207e00	4.6231e00
Schwefel 2.22	Mean	<b>1.4767e-46</b>	1.2455e-15	2.672e-01	3.9218e03
	StdDev	<b>6.1958e-46</b>	9.7600e-17	7.690e-01	5.0525e02
Schwefel 2.21	Mean	<b>8.5432e-115</b>	2.4731e01	2.1494e01	1.26e-02
	StdDev	<b>4.1846e-114</b>	3.2802e00	7.1633e00	2.80e-03
Levy	Mean	<b>1.4998e-32</b>	4.4509e-16	3.4239e01	1.6999e00
	StdDev	<b>1.1135e-47</b>	6.9267e-17	1.1179e01	1.4384e00
Penalized 1	Mean	<b>1.5705e-32</b>	4.5600e-16	1.07599e01	1.8114e-11
	StdDev	<b>5.5674e-48</b>	7.5544e-17	1.08950e01	4.7946e-11
Penalized 2	Mean	<b>1.3662e-32</b>	4.5336e-16	3.06354e01	1.6208e-10
	StdDev	<b>9.0016e-34</b>	5.9422e-17	1.65191e01	2.0738e-10

Note: ABC = artificial bee colony; BA = bat algorithm; BBO = biogeography-based optimization.

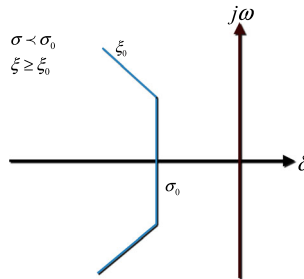


**Figure 7.** The D contour.

The design problem is formulated based on the aforementioned criterion to minimize the multi-objective function  $J$ :

$$J = \sum_{j=1}^{np} \sum_{\delta_{ij} \geq \delta_o} (\delta_o - \delta_{ij})^2 + q \sum_{j=1}^{np} \sum_{\zeta_{ij} \leq \zeta_o} (\zeta_o - \zeta_{ij})^2 \tag{16}$$

subject to the following constraints:

$$0.01 \leq K_{si} \leq 100 \tag{17}$$

$$0.01 \leq T_{1i} \leq 2 \tag{18}$$

$$0.01 \leq T_{2i} \leq 2 \tag{19}$$

$$0.01 \leq T_{3i} \leq 2 \tag{20}$$

$$0.01 \leq T_{4i} \leq 2 \tag{21}$$

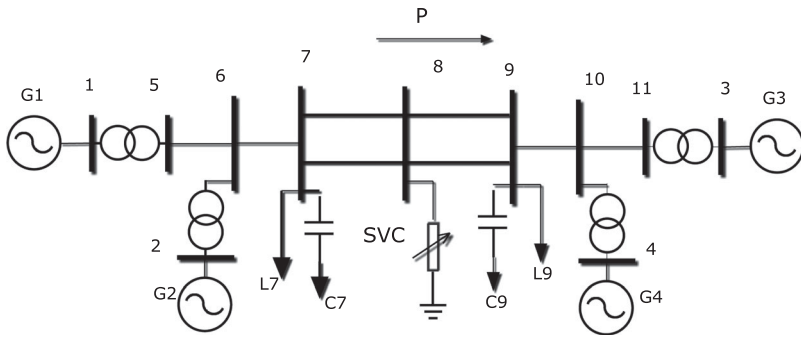


**Figure 8.** Two-area four-machines power system.

**Table 3.** Operating conditions.

Operating condition	Description
Case1	Base case (all lines in service)
Case2	Single line between 7 and 8 out of service
Case3	Single line between 8 and 9 out of service
Case4	Single line between 7 and 9 out of service

where  $i$  denotes the number of controllers, which is five in this study;  $np$  is the number of operating conditions considered in the design process; and  $\sigma_{ij}$  and  $\zeta_{ij}$  are, respectively, the real part and the damping ratio of the  $i$ th eigenvalue of the  $j$ th operating point.

## 6. Results and simulation

The TAFM system, as shown in Figure 8, is a well-known benchmark for power system controller design, testing and comparisons of the damping efficiency. The system is composed of two areas linked through a weak transmission line that allows a 400 MW active power to flow from area 1 to area 2. The data for the system are available in Kundur, Balu, and Lauby (1994).

In controller design, four operating conditions (Table 3) are considered (Eslami *et al.* 2012) to achieve a robust performance during frequent disturbances that occur during system operation.

### 6.1. Optimal SVC location selection

The optimal location of the SVC is selected using the effect of line outage on the system voltages (Abd-Elazim and Ali 2012). As indicated in Table 4, the voltage at bus 8 is largely affected by the line outages, especially in Case4, where the voltage at the bus drops significantly from 0.9647 pu to 0.787828 pu. Hence, bus 8 is the suitable location for installing the SVC, and this accords with the results reported by Martins and Lima (1989). The line current between buses 9 and 10 is selected as the input for SVC since it has high observability to the inter-area mode (Kundur, Balu, and Lauby 1994).

### 6.2. PSS and SVC tuning using the CLBAT

The CLBAT is applied to simultaneously tune the 25 parameters of the four PSSs installed in the generators and the SVC. All operating conditions are considered in the design stage to guarantee optimal damping during all possible conditions and ensure the robustness of the controlled system during variations. The obtained parameters of the controllers are listed in Table 5. Besides CLBAT's

**Table 4.** Effect of line outage on load bus voltages.

Case	Base case	Outage of line 7–8	Outage of line 8–9	Outage of line 7–9
Bus 5	1.0079	1.0036	1.004	0.99702
Bus 6	0.98156	0.971	0.97199	0.95499
Bus 7	0.9672	0.94821	0.95	0.91952
Bus 8	0.9647	<b>0.9242</b>	<b>0.90925</b>	<b>0.78728</b>
Bus 9	1.0044	0.99217	0.9905	0.96632
Bus 10	1.0086	1.0017	1.0008	0.98727
Bus 11	1.0228	1.0201	1.0197	1.0143

**Table 5.** Parameters of the proposed controllers for the comprehensive learning bat algorithm (CLBAT) and bat algorithm (BA).

	CLBAT					BA				
	$K_s$	$T_1$	$T_2$	$T_3$	$T_4$	$K_s$	$T_1$	$T_2$	$T_3$	$T_4$
SVC	1.0025	0.0122	0.0227	0.0122	1.4295	2.1800	0.0206	1.9122	0.0275	0.9218
G1	25.3641	1.4867	1.9919	1.9895	0.0113	96.2402	0.5174	1.6257	1.1438	0.9844
G2	7.8495	1.9972	1.8867	1.9947	0.0211	34.6806	0.6349	1.1051	1.7734	0.0206
G3	11.0329	0.0693	0.0328	1.9988	0.0456	98.6927	0.4037	0.1951	1.9751	1.5256
G4	20.0696	1.9911	1.9914	1.9972	0.0125	40.7534	0.9672	0.7700	1.2238	0.0206

Note: SVC = structured singular value;  $K_s$  = stabilizer gain.

superior accuracy and robustness, the CLBAT controller gains are lower than those of the BA, which is another practical advantage in the realization of the controllers.

### 6.2.1. Optimization performance statistics

To explore the reliability of each algorithm in minimizing the given objective function, the experiment was repeated over 10 runs. The best, worst and average costs at each iteration based on 10 runs are indicated in Figure 9. The statistics in this section were obtained based on an ordinary computer with four CPUs of 3.2 GHz. The optimal design of the controllers' parameters requires observation of the system behaviour, which is carried out in an offline stage; hence, the optimality of the solution is more important than the optimization time. The running time for one iteration of the CLBAT is 39.0262 s versus 19.7331 s for the BA. However, it is the call of the power system analysis toolbox (PSAT) that is computationally heavy, and especially so for the CLBAT (39.0248 s) compared to the BA (19.7325 s) owing to the introduced improvements. This time is mainly due to the communication and parameter settings for the PSAT, as well as the load flow and eigenanalysis operations. Notice that the PSAT is called according to the population for the BA, and twice that number for the CLBAT. The real average computation time of the optimization process per iteration is really negligible compared to the PSAT computations; this value is 1.4 ms for the CLBAT and 0.6 ms for the BA. However, the CLBAT successfully reaches the desired settings for the controllers with the optimum required solution, while the best fitness value of the BA is 1.7917. The CLBAT is also more reliable than the BA in solving the optimization problem, since all 10 runs successfully converge to a solution, as depicted in Figure 9.

### 6.3. Eigenanalysis

The eigenvalues of the system without the controllers are listed in Table 6 for all the operating conditions. It can be clearly seen that the inter-area mode (in bold) is unstable since it has a negative damping ratio for all cases. Moreover, the two local modes are stable but close to the margin of the  $s$ -plane, with insufficient damping ratios around 12% and 8% for all cases. The proposed controllers greatly improve the damping, as indicated by the resulting eigenvalues shown in Table 7. Moreover, the CLBAT-tuned controllers (CLBAT-Cs) outperform the original BA-tuned controllers (BA-Cs) for all cases and for all electromechanical modes. In particular, the inter-area mode is successfully stabilized, with an acceptable damping ratio greater than 58% for all cases. The damping of the local modes

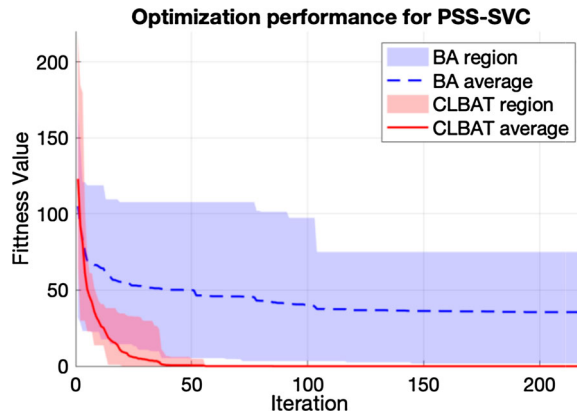


**Figure 9.** Convergence of comprehensive learning bat algorithm (CLBAT) and bat algorithm (BA). PSS = power system stabilizer; SVC = static VAR compensator.

**Table 6.** Open loop system eigenvalues, damping ratios and frequencies.

	Eigenvalues	Damping ratio (%)	Frequency (Hz)
Case1	<b>0.0085 ± j 3.2858</b>	<b>-0.2570</b>	<b>0.5230</b>
	-0.8451 ± j 6.5551	12.7870	1.0430
	-0.5353 ± j 6.6360	8.0400	1.0560
Case2	<b>0.1883 ± j 2.4619</b>	<b>-7.6280</b>	<b>0.3920</b>
	-0.8531 ± j 6.5426	12.9300	1.0410
	-0.5394 ± j 6.5892	8.1590	1.0490
Case3	<b>0.1915 ± j 2.4601</b>	<b>-7.7610</b>	<b>0.3920</b>
	-0.8541 ± j 6.5399	12.9500	1.0410
	-0.5385 ± j 6.5917	8.1430	1.0490
Case4	<b>0.3974 ± j 1.3435</b>	<b>-28.3650</b>	<b>0.2140</b>
	-0.8455 ± j 6.5270	12.8470	1.0390
	-0.5434 ± j 6.5383	8.2820	1.0410

**Table 7.** Eigenvalues, damping ratios and frequencies of the system with comprehensive learning bat algorithm-tuned controllers (CLBAT-Cs) and bat algorithm-tuned controllers (BA-Cs).

	CLBAT-Cs			BA-Cs		
	Eigenvalues	Damping ratio (%)	Frequency (Hz)	Eigenvalues	Damping ratio (%)	Frequency (Hz)
Case1	<b>-3.2501 ± j 4.0152</b>	<b>62.9160</b>	<b>0.6390</b>	<b>-2.0728 ± j 2.9066</b>	<b>58.0620</b>	<b>0.4630</b>
	-7.2855 ± j 9.3981	61.2680	1.4960	-2.0197 ± j 9.9362	19.9190	1.5810
	-6.5611 ± j 9.9040	55.2270	1.5760	-3.8776 ± j 11.5054	31.9370	1.8310
Case2	<b>-3.7421 ± j 2.9490</b>	<b>78.5430</b>	<b>0.4690</b>	<b>-2.0079 ± j 3.1667</b>	<b>53.5500</b>	<b>0.5040</b>
	-7.7259 ± j 9.3368	63.7510	1.4860	-2.7296 ± j 10.0837	26.1290	1.6050
	-6.3177 ± j 9.6433	54.8010	1.5350	-3.2763 ± j 10.8879	28.8150	1.7330
Case3	<b>-2.3849 ± j 3.3077</b>	<b>58.4840</b>	<b>0.5260</b>	<b>-1.4554 ± j 2.7237</b>	<b>47.1270</b>	<b>0.4330</b>
	-6.8595 ± j 9.2610	59.5200	1.4740	-2.4959 ± j 9.4909	25.4330	1.5110
	-6.3334 ± j 10.098	53.1320	1.6070	-3.6723 ± j 11.2435	31.0470	1.7890
Case4	<b>-2.5775 ± j 2.7228</b>	<b>68.7450</b>	<b>0.4330</b>	<b>-0.8586 ± j 3.7061</b>	<b>22.5700</b>	<b>0.5900</b>
	-6.0772 ± j 9.4128	54.2410	1.4980	-1.5742 ± j 7.8216	19.7310	1.2450
	-7.4849 ± j 9.5150	61.8270	1.5140	-2.5815 ± j 11.1819	22.4940	1.7800

is further increased by CLBAT-C achieving values above 50% for all cases compared to just below 32% achieved by the BA-C. Moreover, the damping of the inter-area mode with CLBAT-C is better than the state-of-the-art results in Eslami *et al.* (2012) for the same system and operating conditions.

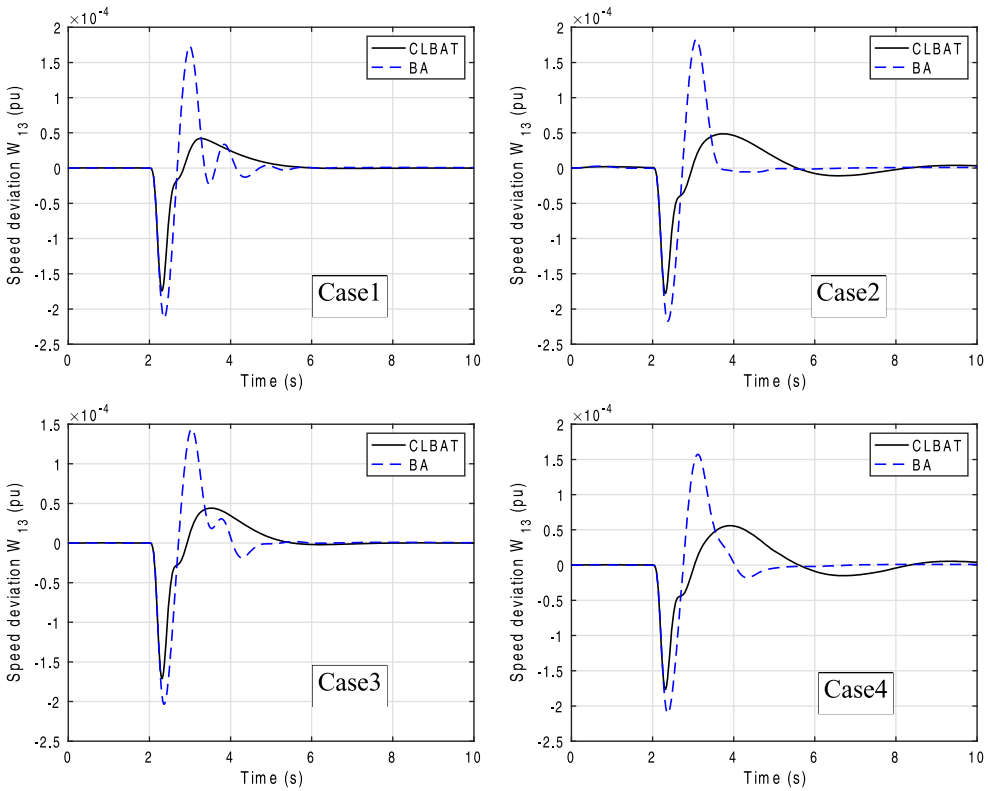


**Figure 10.** Response of  $\omega_{13}$  for a 0.1 pu step increase in  $V_{ref}$  under all cases. CLBAT = comprehensive learning bat algorithm; BA = bat algorithm.

#### 6.4. Nonlinear time-domain simulation

Nonlinear simulation is performed on the nonlinear system to evaluate the performance of the proposed controllers considering a small disturbance of a step increase of 0.1 pu in the reference voltage (Wang *et al.* 2018) of generator 1 at 2 s with duration of 100 ms for all four operating cases, in addition to a three-cycle three-phase fault applied at bus 9 for all cases, which is considered a large disturbance.

Figure 10 illustrates that the CLBAT-Cs outperform the BA-Cs in terms of the oscillation overshoot and the settling times for all the operating cases under the considered small disturbance.

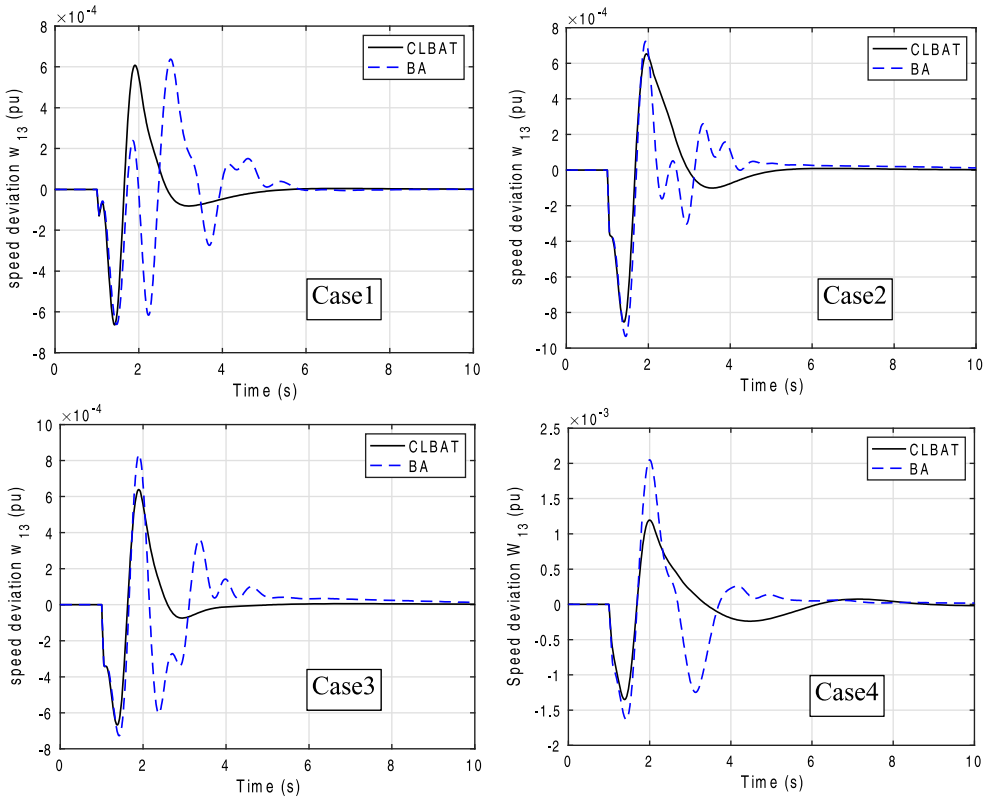
Figure 11 depicts the response of  $\omega_{13}$  during three-cycle three-phase faults at bus 9 for all cases. While both BA-Cs and CLBAT-Cs maintain the system stability and restore the destined operation, the CLBAT-Cs improve the damping compared to the BA-Cs. Superior damping results are achieved in terms of the smallest oscillation amplitude, rapid damping and short settling time.

Moreover, these results are consistent with the eigenvalue analysis of the system, and further demonstrate the capability of CLBAT-Cs to provide high damping to electromechanical oscillations.

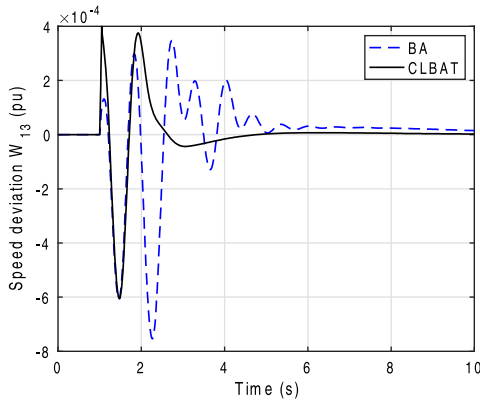
To further validate the performance of the proposed controllers, a different operating condition is considered that corresponds to a light loading condition in which the transferred power from area 1 to area 2 is decreased to 3.5086 pu; then, a three-cycle three-phase fault is applied on bus 9 at  $t = 1$  s.

Figure 12 confirms the superiority of the CLBAT-Cs since the settling time and maximum overshoot are smaller than those of the system response with the BA-Cs.





**Figure 11.** Response of  $w_{13}$  for a three-cycle three-phase fault at bus 9 under all cases. CLBAT = comprehensive learning bat algorithm; BA = bat algorithm.



**Figure 12.** Response of  $w_{13}$  for a three-cycle three-phase fault at bus 9 under light loading conditions. CLBAT = comprehensive learning bat algorithm; BA = bat algorithm.

**Table 8.** Performance indices for a three-cycle three-phase fault for comprehensive learning bat algorithm-tuned controllers (CLBAT-Cs) and bat algorithm-tuned controllers (BA-Cs).

Case	ISE		ITAE	
	CLBAT-Cs	BA-Cs	CLBAT-Cs	BA-Cs
Case1	2.4334e-07	3.8104e-07	0.0014	0.0027
Case2	4.4770e-07	4.5871e-07	0.0021	0.0027
Case3	2.8188e-07	5.1877e-07	0.0013	0.0036
Case4	1.4475e-06	3.1808e-06	0.0058	0.0077

Note: ISE = integral square error; ITAE = integral of the time-weighted absolute error.

## 6.5. Performance indices

The robustness of the CLBAT-Cs is measured based on the integral of the time-weighted absolute error (ITAE) and the integral square error (ISE):

$$\text{ITAE} = \int_{t=0}^{T_{\text{sim}}} t |\Delta\omega_{13}(t)| dt \quad (22)$$

$$\text{ISE} = \int_{t=0}^{T_{\text{sim}}} |\Delta\omega_{13}(t)|^2 dt \quad (23)$$

where  $T_{\text{sim}}$  is the simulation time of the system, set as 10 s. The smaller the values of these indices, the better the system response.

The values of the two integral performance criteria in Table 8 demonstrate the superiority of the developed CLBAT-optimized designs of the controllers over their BA-based counterparts in maintaining an optimal response of the power system during the different cases.

## 7. Conclusion

In this article, the coordinated tuning of PSSs and SVC over a wide range of operating conditions for a TAFM system using a newly developed algorithm, CLBAT, is proposed. The significant contributions of the CLBAT include a new CLS, a modified ELS and the use of an adaptive search mechanism. This greatly enhances the exploration and exploitation phases by increasing the diversity of the microbats and improving the local search. The proposed CLBAT is first tested on a set of benchmark functions to verify its accuracy and optimization stability compared to other algorithms in the literature. CLBAT is then deployed for the optimal design of the PSS and SVC controllers for the TAFM system through optimal relocation of oscillation modes considering four operating conditions. Simulation results, eigenvalue analysis and performance indices confirm the effectiveness of the CLBAT-based controllers in providing sufficient damping during various system disturbances across many operating cases. Future work will focus on the design of wide area controllers of very large-scale power systems based on global signals rather than local signals.

## Disclosure statement

No potential conflict of interest was reported by the authors.

## References

- Abd-Elazim, S. M., and E. S. Ali. 2012. "Coordinated Design of PSSs and SVC via Bacteria Foraging Optimization Algorithm in a Multimachine Power System." *International Journal of Electrical Power & Energy Systems* 41 (1): 44–53.
- Abd-Elazim, S. M., and E. S. Ali. 2016a. "Load Frequency Controller Design via BAT Algorithm for Nonlinear Interconnected Power System." *International Journal of Electrical Power & Energy Systems* 77: 166–177.

- Abd-Elazim, S. M., and E. S. Ali. 2016b. "Optimal Power System Stabilizers Design via Cuckoo Search Algorithm." *International Journal of Electrical Power & Energy Systems* 75: 99–107.
- Abdel-Magid, Y. L., and M. A. Abido. 2003. "Optimal Multiobjective Design of Robust Power System Stabilizers Using Genetic Algorithms." *IEEE Transactions on Power Systems* 18 (3): 1125–1132.
- Abdelaziz, A. Y., and E. S. Ali. 2015. "Static VAR Compensator Damping Controller Design Based on Flower Pollination Algorithm for a Multi-machine Power System." *Electric Power Components and Systems* 43 (11): 1268–1277.
- Abido, M. A., and Y. L. Abdel-Magid. 2003. "Coordinated Design of a PSS and an SVC-Based Controller to Enhance Power System Stability." *International Journal of Electrical Power & Energy Systems* 25 (9): 695–704.
- Bahmani-Firouzi, B., and R. Azizpanah-Abarghoee. 2014. "Optimal Sizing of Battery Energy Storage for Micro-grid Operation Management Using a New Improved bat Algorithm." *International Journal of Electrical Power & Energy Systems* 56: 42–54.
- Bian, X. Y., Y. Geng, K. L. Lo, Y. Fu, and Q. B. Zhou. 2016. "Coordination of PSSs and SVC Damping Controller to Improve Probabilistic Small-Signal Stability of Power System with Wind Farm Integration." *IEEE Transactions on Power Systems* 31 (3): 2371–2382.
- Bouchama, Z., N. Essounbouli, M. N. Harmas, A. Hamzaoui, and K. Saoudi. 2016. "Reaching Phase Free Adaptive Fuzzy Synergetic Power System Stabilizer." *International Journal of Electrical Power & Energy Systems* 77: 43–49.
- Castellanos, R. B., A. R. Messina, and H. U. Sarmiento. 2008. "A  $\mu$ -Analysis Approach to Power System Stability Robustness Evaluation." *Electric Power Systems Research* 78 (2): 192–201.
- Darabian, M., S. M. Mohseni-Bonab, and B. Mohammadi-Ivatloo. 2015. "Improvement of Power System Stability by Optimal SVC Controller Design Using Shuffled Frog-Leaping Algorithm." *IETE Journal of Research* 61 (2): 160–169.
- de Campos, V. A. F., J. J. da Cruz, and L. C. Zanetta Jr. 2014. "Robust Control of Electrical Power Systems Using PSSs and Bilinear Matrix Inequalities." *International Journal of Electrical Power & Energy Systems* 62: 10–18.
- Eslami, M., H. Shareef, A. Mohamed, and M. Khajezadeh. 2012. "An Efficient Particle Swarm Optimization Technique with Chaotic Sequence for Optimal Tuning and Placement of PSS in Power Systems." *International Journal of Electrical Power & Energy Systems* 43 (1): 1467–1478.
- Farah, Anouar, Tawfik Guesmi, and Hsan Hadj Abdallah. 2017. "A New Method for the Coordinated Design of Power System Damping Controllers." *Engineering Applications of Artificial Intelligence* 64: 325–339.
- Gao, W., F. T. Chan, L. Huang, and S. Liu. 2015. "Bare Bones Artificial Bee Colony Algorithm with Parameter Adaptation and Fitness-Based Neighborhood." *Information Sciences* 316: 180–200.
- Ho, Y. C., and D. L. Pepyne. 2002. "Simple Explanation of the No-Free-Lunch Theorem and Its Implications." *Journal of Optimization Theory and Applications* 115 (3): 549–570.
- Hussein, T., M. S. Saad, A. L. Elshafei, and A. Bahgat. 2010. "Damping Inter-area Modes of Oscillation Using an Adaptive Fuzzy Power System Stabilizer." *Electric Power Systems Research* 80 (12): 1428–1436.
- Jalili, S., Y. Hosseinzadeh, and N. Taghizadieh. 2016. "A Biogeography-Based Optimization for Optimum Discrete Design of Skeletal Structures." *Engineering Optimization* 48 (9): 1491–1514.
- Karaboga, D., and B. Basturk. 2007. "A Powerful and Efficient Algorithm for Numerical Function Optimization: Artificial Bee Colony (ABC) Algorithm." *Journal of Global Optimization* 39 (3): 459–471.
- Kundur, P., N. J. Balu, and M. G. Lauby. 1994. *Power System Stability and Control*. Vol. 7. New York: McGraw-Hill.
- Liang, Jing J., A. K. Qin, P. N. Suganthan, and S. Baskar. 2006. "Comprehensive Learning Particle Swarm Optimizer for Global Optimization of Multimodal Functions." *IEEE Transactions on Evolutionary Computation* 10 (3): 281–295.
- Liu, Q., L. Wu, W. Xiao, F. Wang, and L. Zhang. 2018. "A Novel Hybrid Bat Algorithm for Solving Continuous Optimization Problems." *Applied Soft Computing* 73: 67–82.
- Mahabuba, A., and M. A. Khan. 2009. "Small Signal Stability Enhancement of a Multi-machine Power System Using Robust and Adaptive Fuzzy Neural Network-Based Power System Stabilizer." *European Transactions on Electrical Power* 19 (7): 978–1001.
- Mallick, R., R. Ganguli, and M. S. Bhat. 2015. "Robust Design of Multiple Trailing Edge Flaps for Helicopter Vibration Reduction: A Multi-objective Bat Algorithm Approach." *Engineering Optimization* 47 (9): 1243–1263.
- Martins, N., and L. T. G. Lima. 1989. "Determination of Suitable Locations for Power System Stabilizers and Static VAR Compensators for Damping Electromechanical Oscillations in Large Scale Power Systems." *IEEE Transactions on Power Systems* 5 (4): 1455–1469.
- Meng, X. B., X. Z. Gao, Y. Liu, and H. Zhang. 2015. "A Novel Bat Algorithm with Habitat Selection and Doppler Effect in Echoes for Optimization." *Expert Systems with Applications* 42 (17–18): 6350–6364.
- Mondal, D., A. Chakrabarti, and A. Sengupta. 2012. "Optimal Placement and Parameter Setting of SVC and TCSC Using PSO to Mitigate Small Signal Stability Problem." *International Journal of Electrical Power & Energy Systems* 42 (1): 334–340.
- Nechadi, E., M. N. Harmas, A. Hamzaoui, and N. Essounbouli. 2012. "Type-2 Fuzzy Based Adaptive Synergetic Power System Control." *Electric Power Systems Research* 88: 9–15.
- Oshaba, A. S., E. S. Ali, and S. A. Elazim. 2017. "PI Controller Design for MPPT of Photovoltaic System Supplying SRM via Bat Search Algorithm." *Neural Computing and Applications* 28 (4): 651–667.
- Peres, Wesley, Ivo Chaves Silva Júnior, and João Alberto Passos Filho. 2018. "Gradient Based Hybrid Metaheuristics for Robust Tuning of Power System Stabilizers." *International Journal of Electrical Power & Energy Systems* 95: 47–72.

- Saad, A., Z. Dong, B. Buckham, C. Crawford, A. Younis, and M. Karimi. 2019. "A New Kriging–bat Algorithm for Solving Computationally Expensive Black-box Global Optimization Problems." *Engineering Optimization* 51 (2): 265–285.
- Sambariya, D. K., and R. Prasad. 2015. "Optimal Tuning of Fuzzy Logic Power System Stabilizer Using Harmony Search Algorithm." *International Journal of Fuzzy Systems* 17 (3): 457–470.
- Sauer, P. W., and M. A. Pai. 1998. *Power System Dynamics and Stability*. Vol. 101. Upper Saddle River, NJ: Prentice Hall.
- Shahgholian, G., and A. Movahedi. 2016. "Power System Stabiliser and Flexible Alternating Current Transmission Systems Controller Coordinated Design Using Adaptive Velocity Update Relaxation Particle Swarm Optimisation Algorithm in Multi-machine Power System." *IET Generation, Transmission & Distribution* 10 (8): 1860–1868.
- Simon, D. 2008. "Biogeography-Based Optimization." *IEEE Transactions on Evolutionary Computation* 12 (6): 702–713.
- Talafuse, T. P., and E. A. Pohl. 2016. "A Bat Algorithm for the Redundancy Allocation Problem." *Engineering Optimization* 48 (5): 900–910.
- Tofighi, M., M. Alizadeh, S. Ganjefar, and M. Alizadeh. 2015. "Direct Adaptive Power System Stabilizer Design Using Fuzzy Wavelet Neural Network with Self-Recurrent Consequent Part." *Applied Soft Computing* 28: 514–526.
- Wang, D., N. Ma, M. Wei, and Y. Liu. 2018. "Parameters Tuning of Power System Stabilizer PSS4B Using Hybrid Particle Swarm Optimization Algorithm." *International Transactions on Electrical Energy Systems* 28 (9): e2598.
- Wang, G. G., and Y. Tan. 2017. "Improving Metaheuristic Algorithms with Information Feedback Models." *IEEE Transactions on Cybernetics* 49 (2): 542–555.
- Yang, T. C. 1997. "Applying  $H_\infty$  Optimization Method to Power System Stabilizer Design—Parts 1&2." *International Journal of Electrical Power & Energy Systems* 19 (1): 29–35.
- Yang, Xin-She, and Amir Hossein Gandomi. 2012. "Bat Algorithm: A Novel Approach for Global Engineering Optimization." *Engineering Computations* 29 (5): 464–483.
- Zhan, Z. H., J. Zhang, Y. Li, and H. S. H. Chung. 2009. "Adaptive Particle Swarm Optimization." *IEEE Transactions on Systems, Man, and Cybernetics, Part B (Cybernetics)* 39 (6): 1362–1313.

## Appendix

CLBAT:  $\alpha = 0.98$ ,  $\gamma = 0.98$ ,  $A = 1.8$ ,  $r = 0.8$ ,  $f_{\max} = 2$ ,  $f_{\min} = 0$ ,  $W_{\max} = 0.9$ ,  $W_{\min} = 0.2$ ,  $P_{c_{\max}} = 0.8$ ,  $P_{c_{\min}} = 0.2$ ,  $G = 40$ .

BA:  $\alpha = 0.9$ ,  $\gamma = 0.9$ ,  $A = 1$ ,  $r = 0.8$ ,  $f_{\max} = 1$ ,  $f_{\min} = 0$ .

Excitation system:  $K_A = 155$ ,  $T_A = 0.055$  s,  $K_f = 0.125$ ,  $T_f = 1.8$  s,  $K_E = 1$ ,  $T_E = 1$  s,  $T_r = 0.05$  s,  $S_E = f(E_{fd}) = 0.0056 (e^{(1.075|E_{fd}|)} - 1)$ .

SVC controller:  $T_r = 0.02$  s,  $K_r = 10$ .